

# Microdisplacement Printing

A. A. Dameron, J. R. Hampton, R. K. Smith, T. J. Mullen, S. D. Gillmor, and P. S. Weiss\*

*Departments of Chemistry and Physics, 104 Davey Laboratory,  
The Pennsylvania State University, University Park, Pennsylvania 16802*

*Received May 25, 2005; Revised Manuscript Received July 25, 2005*

## ABSTRACT

We describe a new patterning technique that employs microcontact printing to replace preformed labile self-assembled monolayers (SAMs) selectively; we call this “microdisplacement printing”. We demonstrate that this technique results in ordered molecular regions of both the patterning (“displacing”) molecule as well as the remnant labile film, here 1-adamantanethiolate. The existence of the 1-adamantanethiolate SAM before patterning hinders lateral surface diffusion of the patterning molecules, and therefore permits the use of molecules that are otherwise too mobile to pattern by other methods.

Microcontact printing ( $\mu$ CP) has been proposed for applications such as microelectronics,<sup>1–3</sup> chemical and biological sensing,<sup>4–6</sup> biologically compatible surfaces,<sup>7,8</sup> and micro-fabrication<sup>9,10</sup> because of the rapid and straightforward methodology that produces high-resolution patterns over large printing areas.<sup>11–13</sup> However, as discussed in previous reports,<sup>14–16</sup> one limitation of  $\mu$ CP is the lateral spreading of the molecules used for patterning (“ink”) across the substrate surface during the time the stamp is in contact with the substrate. Here, we demonstrate a technique we call “microdisplacement printing” ( $\mu$ DP), in which relatively weakly bound and thus labile 1-adamantanethiolate (AD) self-assembled monolayers (SAMs) are selectively replaced with more strongly bound molecules to create patterned SAMs. By manipulating competitive adsorption to pattern SAMs, the problems associated with lateral surface diffusion and molecular exchange during patterning can be circumvented.

Microcontact printing is the patterning of a substrate by contact (“stamping”) with a “molecularly inked” elastomeric stamp. A great deal of attention has been placed on  $\mu$ CP of alkanethiol molecules on gold substrates,<sup>10,14–16</sup> although many other systems have been studied. Lateral surface diffusion rates increase with decreasing alkyl chain length;<sup>9,17,18</sup> thus, short chain alkanethiolates and other low-molecular-weight molecules are particularly susceptible to such diffusion during the patterning process and thus dissolution of the patterns. This lateral mobility increases if no molecule is used to fill in the empty spaces (a process called backfilling) where no pattern is present on the substrate. In addition, although some solvent presence may be necessary for ordering the patterned molecules, prolonged exposure to solvent during backfilling steps enables the mobility of the

patterned molecules at the pattern interfaces, and furthermore promotes molecular exchange of the patterned molecules for backfilling molecules.

These problems can be avoided by an alternate patterning technique, microdisplacement printing, which uses a preassembled monolayer that is well ordered to protect the surface, but is sufficiently labile such that other molecules can displace it through competitive adsorption. Stamping on such a surface directs the molecules to adsorb where their local concentration is highest and holds the ink molecules in place once adsorbed during the stamping procedure. This procedure also limits the need for solution processing because the unpatterned regions are prefilled. Here, we demonstrate  $\mu$ DP with both 1-decanethiol (C10) and 11-mercaptoundecanoic acid (MUDA). Trends in the degree of displacement were explored by stamping with unpatterned poly(dimethylsiloxane) (PDMS) stamps for a variety of displacement times and ink concentrations. This information was used to choose appropriate times and concentrations for patterned samples.

All of the patterned samples were fabricated and subsequently imaged with scanning tunneling microscopy (STM) or lateral force microscopy (LFM). As demonstrated previously (also see the Supporting Information), AD forms well-ordered hexagonally close-packed one-molecule-thick films on Au{111}, with a nearest-neighbor packing distance of  $6.9 \pm 0.4 \text{ \AA}$ .<sup>19</sup> Adamantanethiolate films are labile, in that it is possible to displace the AD molecules from the surface by submersion of the sample into a solution of a different thiolated molecule such as an *n*-alkanethiol. However, submersion of a preassembled *n*-alkanethiolate SAM into an AD solution results in little or no displacement. This property can be applied to backfilling of traditional  $\mu$ CP samples. LFM imaging of a Au{111} substrate that has been patterned using  $\mu$ CP methods and then backfilled with AD shows a

\* Corresponding author. E-mail: stm@psu.edu.

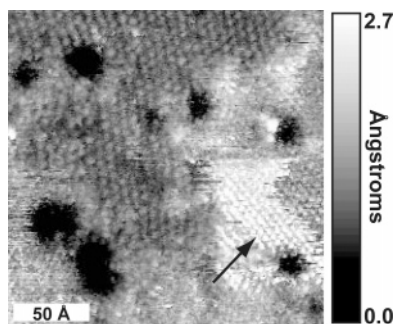


**Figure 1.** Scanning tunneling microscopy image of a two-component, self-assembled monolayer of 1-adamantanethiolate and 1-decanethiolate, fabricated by microdisplacement printing. The ordered lattices of both components can be seen; the more protruding self-assembled monolayer domains with the smaller lattice spacing (arrow) are 1-decanethiolate. The area imaged is  $175 \times 175 \text{ \AA}^2$ , recorded with a sample bias of 1 V and a tunneling current of 4.0 pA.

distinct pattern (see Supporting Information). After printing, the AD molecules adsorb to the gold substrate between the patterned features in the areas where the patterned molecules are not present without disturbing the preexisting molecules. Below, we show that by using the lability of the AD SAMs it is also possible to “fill in” the space between the patterned features *before* patterning via  $\mu$ DP, thus preventing pattern dissolution, even for molecules that would normally diffuse rapidly across the substrate surface.

During  $\mu$ DP, molecules are stamped onto an existing SAM, displacing the SAM only where the stamp meets the surface. Within the contacted area, the displacement is observed first at film and substrate defects in the SAM and then as patches of ordered molecules that increase in surface coverage from their origins at defects. Figure 1 shows a  $175 \times 175 \text{ \AA}^2$  STM image of a sample created by  $\mu$ DP on an AD SAM with an unpatterned PDMS stamp inked with 100 mM C10 for 3.5 min. Large ordered areas of each lattice type are observed where there was only AD previously. It is straightforward to distinguish the two adsorbed molecules because of the differences in lattice size, lattice spacing, and apparent height ( $\Delta h \approx 2.5 \text{ \AA}$ ) between them. The more protruding lattice (lower right indicated by the arrow), juxtaposing two substrate defects, is C10, whereas the less protruding lattice (the majority of the image) is AD.

The extent of displacement can be controlled by tuning the stamping duration and ink concentration during sample fabrication. Figure 2 shows a matrix of STM images of AD SAMs contacted with an unpatterned C10-inked stamp using different combinations of stamping time and stamping ink concentration. In this matrix, the stamping duration increases to the right and the C10-inking solution concentration increases downward. Each sample was imaged with STM and a representative  $1000 \times 1000 \text{ \AA}^2$  image was selected for each time and concentration pair. Although there is some variation across each sample due to concentration gradients across the stamp, the degree of contact between the stamp and sample and so forth, the increasing trends are reproducible. It can be seen in the figure that both increasing the stamp duration and increasing the ink concentration increase

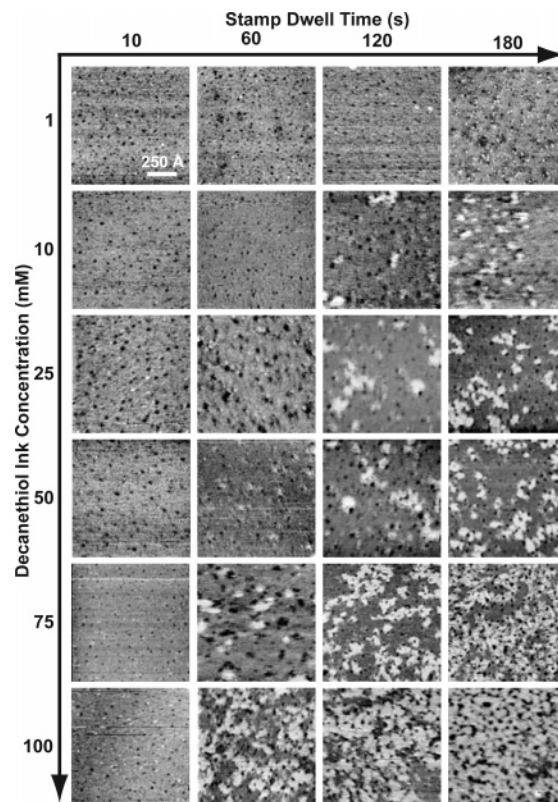


**Figure 2.** Matrix of scanning tunneling microscopy images of microdisplacement printing of a 1-adamantanethiolate self-assembled monolayer with an unpatterned poly(dimethylsiloxane) stamp inked with 1-decanethiol (imaged as protruding features). The concentrations of the 1-decanethiol solution used increase top to bottom, whereas the durations of the stamping process increase left to right. All imaged areas are  $1000 \times 1000 \text{ \AA}^2$ , recorded with a sample bias of 1 V and tunneling currents between 1 and 2 pA.

the displacement. However, it should also be noted that, as in solution displacement, the degree of order of the C10 lattice also increases with increased displacement. For example, at an ink concentration of 100 mM, a 10-s stamping time results in small clusters of C10 molecules dispersed randomly. With increased stamping time, these clusters grow and order into larger patches, and finally C10 domains nearly cover the surface for a 180-s stamping time.

The coverage is shown quantitatively in Figure 3, where the mean fractional coverage of C10 lattice is plotted as a function of stamping time (A) and ink concentration (B). The mean fractional coverages were extracted from a set of STM images for each sample and were determined by counting the number of pixels above a height threshold and dividing them by the total number of pixels in the image. Images were taken from different areas across the samples, and the resulting fractions were averaged. Images were  $1000 \times 1000 \text{ \AA}^2$  and did not include Au{111} step edges. As observed in Figure 2, the coverage increases with both stamp time and ink concentration. Furthermore, for each concentration there is a time below which there is little displacement. This time decreases with increasing concentration (i.e., for each stamping time there is also a concentration below which there is little displacement). This behavior is likely due to

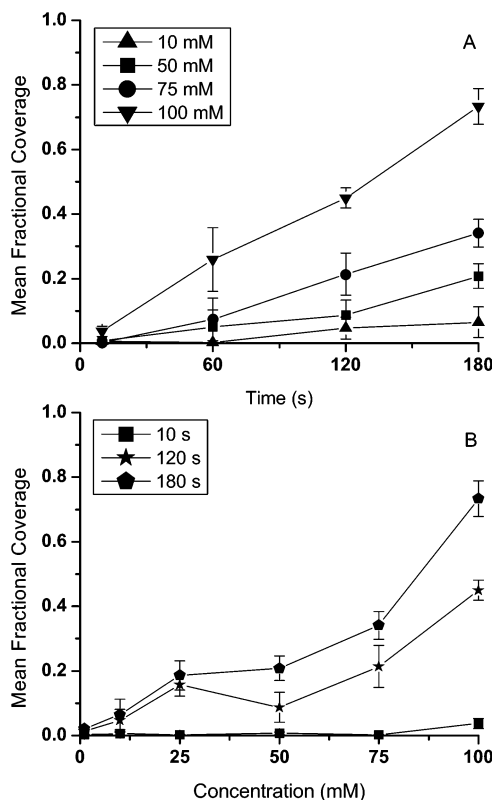


**Figure 3.** Plots of the mean fractional coverage of 1-decanethiolate in scanning tunneling microscopy images of microdisplacement printed samples, (A) as a function of stamp time and (B) as a function of ink concentration. Each data point was averaged from a series of images that have areas of  $1000 \times 1000 \text{ \AA}^2$ , were recorded with a sample bias of 1 V and tunneling currents between 1 and 2 pA.

the ink transport from the stamp to the surface through the existing monolayer. Although the unpatterned stamp contacts the surface everywhere, the C10-ink adsorption is limited by the existing AD SAM, initially resulting in C10 patches at and about AD SAM defects. The longer the stamp contacts the surface and the higher the concentration of the ink on the stamp, the more the ink molecules have a chance to disrupt the AD SAM. As observed in other displacement studies, the limiting step is the initial removal and replacement of the preexisting monolayer.<sup>19,20</sup> Using these observed trends, we are able to optimize  $\mu$ DP; determining the detailed kinetics of the displacement process requires substantially greater statistics so as to be comparable with ensemble-averaging methods.<sup>21–24</sup>

Using the data shown in Figures 2 and 3 for stamping with an unpatterned stamp, we can estimate the stamping times and ink concentrations for analogous stamping with a patterned stamp. In the case of pattern stamping, initially MUDA was used because the difference between the terminal functionalities for the MUDA and AD pair results in higher LFM contrast than for the C10 and AD pair. Displacement of AD by stamped MUDA is expected to follow trends similar to those observed for AD and C10 in Figures 2 and 3.

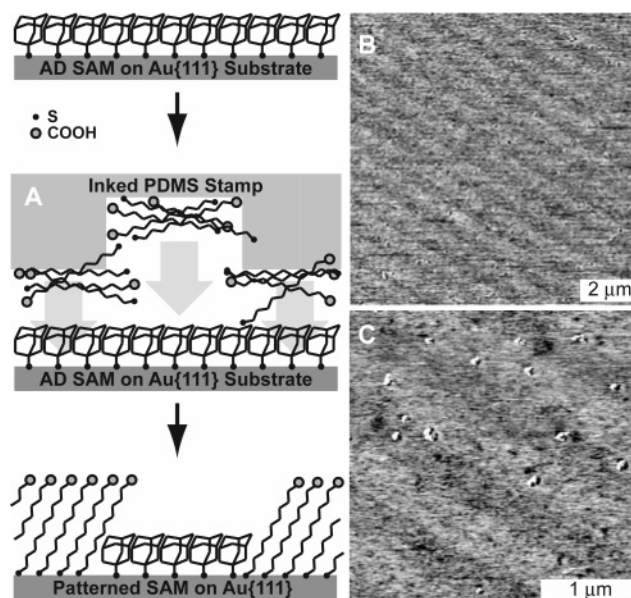


**Figure 4.** (A) Schematic depicting microdisplacement printing on a 1-adamantanethiolate self-assembled monolayer with an 11-mercaptoundecanoic acid-inked stamp. A 1-adamantanethiolate self-assembled monolayer is first formed on gold by solution deposition for 24 h. Then, the molecularly inked stamp is contacted directly onto the 1-adamantanethiolate, resulting in patterned regions of both 1-adamantanethiolate and 11-mercaptoundecanoic acid that mirror the relief pattern on the stamp. Note that the schematic is not to scale. (B and C) Lateral force microscopy images of patterned Au{111} made by microdisplacement printing using a 1200 lines/mm poly(dimethylsiloxane) stamp inked with a 25 mM 11-mercaptoundecanoic acid solution (3 min stamp–substrate contact time). The high-friction (shown as light) stripes are the stamped 11-mercaptoundecanoic acid and the low-friction (shown as dark) stripes are the 1-adamantanethiolate self-assembled monolayer. (B) Lateral force micrograph of a  $10 \times 10 \mu\text{m}^2$  area, recorded at a scan rate of 2 Hz with a force setpoint of 0.5 nN. (C) Lateral force micrograph of a  $3 \times 3 \mu\text{m}^2$  area, recorded at a scan rate of 2 Hz with a force setpoint of 0.5 nN.

Figure 4 demonstrates  $\mu$ DP patterning using 25 mM MUDA on a 1200 lines/mm PDMS stamp. As in the unpatterned case, the stamp was contacted directly to a previously assembled AD SAM. The MUDA molecules displaced the AD molecules where the stamp contacted the sample (along the lines in the PDMS stamp), creating patterned lines of MUDA. The limited contrast between the AD and MUDA stripes in Figure 4 is likely caused by incomplete displacement of the AD SAM by MUDA. We have extended this technique successfully to other molecules including molecules that are too mobile on the surface to pattern by conventional  $\mu$ CP, specifically short chain alkanethiols. Figure 5 shows patterned SAMs created by  $\mu$ DP using C10. In both cases, the regions of AD and C10 replicate the stamp geometry. The existence of a pattern that mirrors the stamp indicates that the AD SAM effectively hindered the lateral mobility of C10 outside of the intended displaced regions. In the analogous  $\mu$ CP of C10, no two-component pattern is observed (see Supporting Information). This is consistent with previous  $\mu$ CP data for the dissolution of patterns of chain alkanethiols longer than those used here.<sup>16</sup>

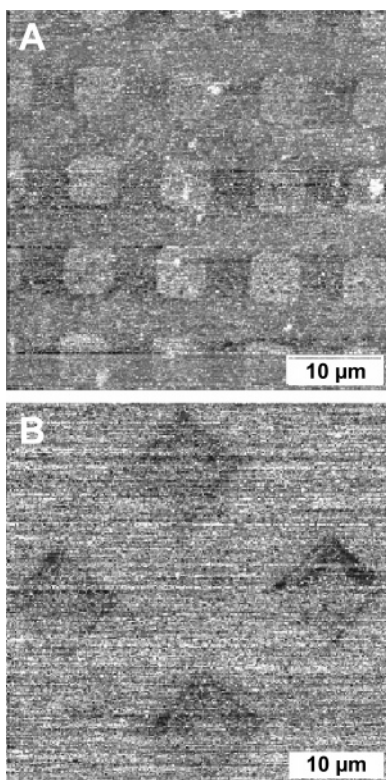


**Figure 5.** (A) Lateral force microscopy image of patterned Au{111} substrate made by microdisplacement printing using a poly(dimethylsiloxane) stamp with 5  $\mu\text{m}$  square wells at a 10  $\mu\text{m}$  pitch that was inked with a 100 mM 1-decanethiol solution for (3 min stamp–substrate contact time). The high-friction (shown as light) squares are the 1-adamantanethiolate self-assembled monolayer and the low-friction (shown as dark) background is the stamped 1-decanethiolate. The imaged area was 40  $\times$  40  $\mu\text{m}^2$ , recorded at a scan rate of 1 Hz at a force setpoint of 1.0 nN. (B) Lateral force microscopy image of a patterned Au{111} substrate made by microdisplacement printing using a poly(dimethylsiloxane) stamp with 10- $\mu\text{m}$  square posts at a 20- $\mu\text{m}$  pitch that was inked with a 25 mM 1-decanethiol solution for (5 min stamp–substrate contact time). The low-friction squares are stamped 1-decanethiolate, and the high-friction background is the 1-adamantanethiolate self-assembled monolayer. The imaged area was 40  $\times$  40  $\mu\text{m}^2$ , recorded at a scan rate of 2 Hz at a force setpoint of 2.0 nN.

Microdisplacement printing increases the sophistication and enhances the precision of traditional  $\mu\text{CP}$  by hindering the mobility of stamped molecules on the substrate surface both during and following the stamping process. The existence of the SAM before stamping blocks lateral movement of the stamped molecules during patterning, something that is not possible by secondary backfilling techniques. As a result, we have increased the library of patternable molecules by adding molecules that are too mobile to pattern by other methods and can also increase the resolution and stability of features patterned by these methods. Traditional  $\mu\text{CP}$  methods often require a solution deposition step, thereby degrading the resolution of the pattern interfaces as well as the composition of the patterns themselves due to molecular exchange. Microdisplacement printing eliminates the need

for solvent exposure after stamping because no backfilling step is required. This exploitation of competitive adsorption for patterning of SAMs can be extended to other self-assembly patterning techniques.

**Acknowledgment.** The authors thank Brent Mantoath for valuable analytical assistance. The Air Force Office of Scientific Research, Army Research Office, Defense Advanced Research Projects Agency, National Science Foundation, Office of Naval Research, and Semiconductor Research Corporation are gratefully acknowledged for their support.

**Supporting Information Available:** Detailed experimental procedures and background on 1-adamantanethiolate SAMs. This material is available free of charge via the Internet at <http://pubs.acs.org>.

## References

- (1) Rogers, J. A.; Bao, Z.; Meier, M.; Dodabalapur, A.; Schueller, O. J. A.; Whitesides, G. M. *Synth. Met.* **2000**, *115*, 5–11.
- (2) Leufgen, M.; Lebib, A.; Muck, T.; Bass, U.; Wagner, V.; Borzenko, T.; Schmidt, G.; Geurts, J.; Molenkamp, L. W. *Appl. Phys. Lett.* **2004**, *84*, 1582–1584.
- (3) Jeon, N. L.; Clem, P. G.; Nuzzo, R. G.; Payne, D. A. *J. Mater. Res.* **1995**, *10*, 2996–2999.
- (4) Mrksich, M.; Whitesides, G. M. *Trends Biotechnol.* **1995**, *13*, 228–235.
- (5) Flink, S.; Schönherr, H.; Vancso, G. J.; Geurts, F. A. J.; van Leerdam, K. G. C.; van Veggel, F. C. J. M.; Reinhoudt, D. N. *J. Chem. Soc., Perkin Trans. 2* **2000**, *2000*, 2141–2146.
- (6) Goh, J. B.; Tam, P. L.; Loo, R. W.; Goh, M. C. *Anal. Biochem.* **2003**, *313*, 262–266.
- (7) Jenkins, A. T. A.; Bushby, R. J.; Evans, S. D.; Knoll, W.; Offenhausser, A.; Ogier, S. D. *Langmuir* **2002**, *18*, 3176–3180.
- (8) Chen, C. S.; Mrksich, M.; Huang, S.; Whitesides, G. M.; Ingber, D. E. *Biotechnol. Prog.* **1998**, *14*, 356–363.
- (9) Delamarche, E.; Geissler, M.; Wolf, H.; Michel, B. *J. Am. Chem. Soc.* **2002**, *124*, 3834–3835.
- (10) Wilbur, J. L.; Kumar, A.; Kim, E.; Whitesides, G. M. *Adv. Mater.* **1994**, *6*, 600–604.
- (11) Xia, Y. N.; Whitesides, G. M. *Angew. Chem., Int. Ed.* **1998**, *37*, 551–575.
- (12) Smith, R. K.; Lewis, P. A.; Weiss, P. S. *Prog. Surf. Sci.* **2004**, *75*, 1–68.
- (13) Kumar, A.; Biebuyck, H. A.; Whitesides, G. M. *Langmuir* **1994**, *10*, 1498–1511.
- (14) Larsen, N. B.; Biebuyck, H.; Delamarche, E.; Michel, B. *J. Am. Chem. Soc.* **1997**, *119*, 3017–3026.
- (15) Libiouille, L.; Bietsch, A.; Schmid, H.; Michel, B.; Delamarche, E. *Langmuir* **1999**, *15*, 300–304.
- (16) Delamarche, E.; Schmid, H.; Bietsch, A.; Larsen, N. B.; Rothuizen, H.; Michel, B.; Biebuyck, H. *J. Phys. Chem. B* **1998**, *102*, 3324–3334.
- (17) Stranick, S. J.; Parikh, A. N.; Allara, D. L.; Weiss, P. S. *J. Phys. Chem.* **1994**, *98*, 11136–11142.
- (18) Poirier, G. E.; Tarlov, M. J.; Rushmeier, H. E. *Langmuir* **1994**, *10*, 3383–3386.
- (19) Dameron, A. A.; Charles, L. F.; Weiss, P. S. *J. Am. Chem. Soc.* **2005**, *127*, 8697–8704.
- (20) Fuchs, D. J. Probing Nanoparticle Assemblies and Substrate Effects on Self-Assembled Monolayers. Ph.D. Thesis, The Pennsylvania State University, University Park, PA, 2004.
- (21) Bensebaa, F.; Voicu, R.; Huron, L.; Ellis, T. H.; Kruus, E. *Langmuir* **1997**, *13*, 5335–5340.
- (22) Bain, C. D.; Troughton, E. B.; Tao, Y. T.; Evall, J.; Whitesides, G. M.; Nuzzo, R. G. *J. Am. Chem. Soc.* **1989**, *111*, 321–335.
- (23) Peterlinz, K. A.; Georgiadis, R. *Langmuir* **1996**, *12*, 4731–4740.
- (24) Subramanian, R.; Lakshminarayanan, V. *Electrochim. Acta* **2000**, *45*, 4501–4509.

NL050981J